♦ PMD Compensation/Mitigation Techniques for High-Speed Optical Transport

Henning Bülow, Chongjin Xie, Axel Klekamp, Xiang Liu, and Bernd Franz

In high-speed long-haul optical transport systems with channel data rates at 40 Gb/s and beyond, polarization mode dispersion (PMD) is one of the major obstacles that limits system performance. It is desired or in most cases required to increase the system tolerance to PMD through PMD compensation and mitigation. In this paper, we review the techniques of PMD compensation and mitigation, including per-channel based optical PMD compensators (PMDCs), analog and digital electronic PMDCs, and all-channel PMD mitigation using distributed fast polarization scrambling and forward error correction (FEC). With the emergence of digital coherent detection, the signal optical field becomes digitally available, enabling powerful digital PMDC techniques to be applied. Digital PMDC techniques in optical single carrier coherent systems and orthogonal frequency division multiplexing (OFDM) systems are briefly reviewed. © 2009 Alcatel-Lucent.

Introduction

In the 1990s, when starting to pursue the increase of the channel rate of optical wavelength division multiplexing (WDM) transmission systems with unrepeatered link lengths of hundreds of kilometers from 2.5 Gb/s to 10 Gb/s, engineers realized that some of the installed fiber links exhibit an optical property that was not considered previously: polarization mode dispersion (PMD) [41, 42]. This effect can lead to strong signal distortion, and system degradation becomes even more likely for 40 Gb/s systems deployed today and future 100 Gigabit Ethernet systems.

Since PMD effects can drift over time [12, 26] and are different for each wavelength channel, several active compensation techniques have been proposed to mitigate the degrading effect of PMD [10, 11]. The majority of these approaches can be classified into optical and electrical compensation techniques that apply optical signal processing within an optical PMD compensator (PMDC) unit or post-detection electronic signal processing of the photodiode signal by an electronic equalizer within the receiver.

In this paper, we review the advances in optical and electronic technologies for PMD mitigation. We first briefly analyze the impact of installed fiber PMD on a transmission system and how to quantify it. The principle and structure of optical PMDCs are described next. The impact of modulation formats on the design of optical PMDCs as well as the performance of a two-stage optical PMDC for 40 Gb/s non-return-to-zero differential phase shift keying (NRZ-DPSK) will be discussed. We follow with a discussion of electronic equalizers, which process the electrical signal provided

Bell Labs Technical Journal 14(1), 105–124 (2009) © 2009 Alcatel-Lucent. Published by Wiley Periodicals, Inc.
Published online in Wiley InterScience (www.interscience.wiley.com). • DOI: 10.1002/bltj.20357

Panel 1. Abbreviations, Acronyms, and Terms

ADC—Analog-to-digital converter
ASIC—Application-specific integrated circuit
BER—Bit error ratio
CD—Chromatic dispersion
CMOS—Complementary metal-oxide semiconductor
CO-OFDM—Coherent optical OFDM
CSRZ—Carrier-suppressed RZ
dB—Decibel
DEP—Depolarization
DFE—Decision feedback equalizer
DGD—Differential group delay
DOP—Degree of polarization
DPSK—Differential phase shift keying
DSP—Digital signal processing
DWDM—Dense wavelength division multiplexing
EDC—Electronic dispersion compensator
EDE—Electronic distortion equalizer
FEC—Forward error correction
FFE—Feed-forward equalizer
FSE—Fractional spaced equalizer
GSa/s—Gigasamples per second
IC—Integrated circuit
I/Q—In-phase/quadrature
ISI—Inter-symbol interference
km—Kilometer
MLSE—Maximum likelihood sequence estimation
ms—Millisecond
NRZ—Non-return-to-zero
OFDM—Orthogonal frequency division multiplexing
OOK—On-off keying
OP—Outage probability
OSNR—Optical signal-to-noise ratio
OTU—Optical transport unit
PBS—Polarization beam splitter
PC—Polarization controller
PCD—Polarization-dependent chromatic dispersion
PDM—Polarization division multiplexed
PM—Polarization maintaining
PMD—Polarization mode dispersion
PMDC—PMD compensator
PMF—Polarization maintaining fiber
PRBS—Pseudo random bit sequence
ps—Picosecond
PS—Polarization scrambler
PSBT—Phase-shifted binary transmission
PSP—Principal state of polarization
QPSK—Quadrature phase shift keying
RF—Radio frequency
rms—Root mean square
RZ—Return-to-zero
SCR—Scrambler
SFI-5—Serdes Framer Interface Level 5
SMF—Single mode fiber
SOP—State of polarization
TS—Training symbols
UFEC—Ultra forward error correction
WDM—Wavelength division multiplexing

by the photodiode in the receiver, and are investigated for PMD mitigation. Analog signal processing will be discussed and compared to processing of digitized signal samples. Then we look more closely at PMD mitigation by distributed polarization scrambling along the transmission link. Compared with the other compensation schemes discussed in this paper, scrambling enables the compensation of all WDM channels simultaneously. We will first describe the operation in principle and then discuss some experimental results gained in lab experiments at 43 Gb/s. We examine the PMD mitigation capability of transmission technologies widely discussed for advanced 40 Gb/s transmission and future 100 Gb/s, e.g., for optical orthogonal frequency division multiplexing (OFDM) transmission systems and for polarization-multiplexed quadrature phase shift keying (QPSK) modulated signals, abbreviated as PDM-QPSK. Both schemes can access optical field information and use analog-to-digital conversion and extensive digital signal processing for signal detection and distortion equalization. We conclude with a summary on PMD compensation performance versus technical complexity of the discussed PMD mitigation schemes.

Impact of PMD on Transmission

The PMD of an optical transmission link mainly arises from variation of the residual optical birefringence along the fiber length, which is induced during the production cabling, and placing of the fiber [42].

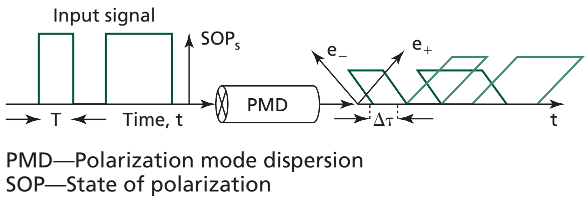

Figure 1.
Optical data signal at the input and output of a fiber having a first-order PMD of Δτ.

Nevertheless, other optical components or sub-systems within the optical signal path might also add to the link PMD, i.e., optical amplifiers, dispersion compensating fiber modules, and wavelength multiplexers.

In first-order approximation, the effect of all these cascaded birefringences can be regarded as a single optical birefringence having a pair of principal states of polarization, PSPs e_- and e_+. They are orthogonally polarized and exhibit different group delays τ_- and τ_+ for slow and fast PSP, respectively. The difference in the group delay is denoted by the differential group delay (DGD) $\Delta\tau = \tau_+ - \tau_-$ (see **Figure 1**).

In the presence of link PMD, the transmitter signal splits among the fast and slow PSP depending on its state of polarization (SOP). The dual path propagation due to the DGD (see Figure 1) leads to a temporal broadening of the bit, and thus to inter-symbol interference (ISI).

Figure 2 shows measurements of the DGD of an installed 246 kilometer (km) fiber link versus time and wavelength. The measurements reveal that DGD as well as PSP vary statistically with wavelength and with time. Therefore PMD is quantified by statistical means: the mean value $\langle\Delta\tau\rangle$ of the DGD—often referred to as the PMD value of a link—and the probability density function of the actual DGD ($\Delta\tau$), which is given by the Maxwellian distribution

$$\rho(\Delta\tau) = \frac{32}{\pi^2}\frac{1}{\langle\Delta\tau\rangle}\left(\frac{\Delta\tau}{\langle\Delta\tau\rangle}\right)^2 \exp\left(-\frac{4}{\pi}\left(\frac{\Delta\tau}{\langle\Delta\tau\rangle}\right)^2\right) \quad (1)$$

under the assumption of an infinitely long fiber with weak mode coupling. Commonly $\langle\Delta\tau\rangle$ and $\rho(\Delta\tau)$ of a fiber are measured by scanning the wavelength while picking DGD samples.

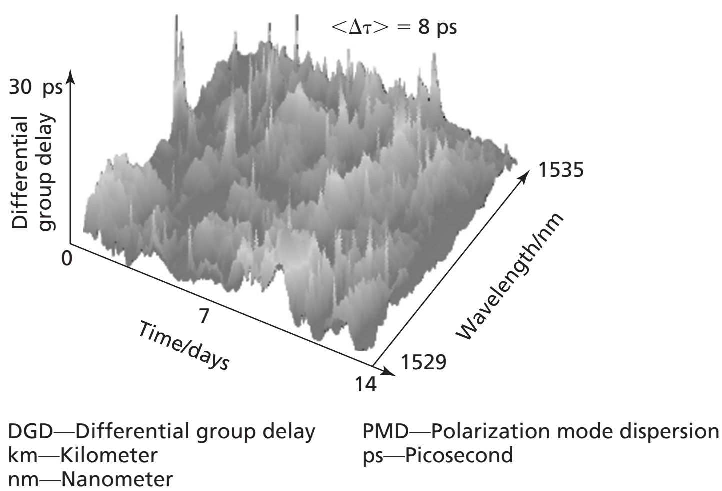

Figure 2.
DGD of an installed fiber (246 km length, 8 ps PMD) measured over a time span of 14 days and a wavelength range of 6 nm.

PMD Tolerance of a System

Variation of DGD ($\Delta\tau$) and PSP with time leads to a variation of the signal distortion and thus a fluctuating bit error rate (BER). Times of poor BER, e.g., BER $> 10^{-3}$ for forward error correction (FEC) supported systems, mean an outage for the transmission system. Due to the statistical nature of PMD, the impact on a transmission system is quantified by the outage probability (OP) for a PMD-induced outage [12].

The robustness of a transmission system to PMD is expressed by the PMD tolerance, i.e., the maximum PMD value ($\langle\Delta\tau\rangle$) of the link that leads to a specific OP given a certain optical signal-to-noise ratio (OSNR) margin. Typical values for OP and margin are 10^{-5} and 2 decibels (dB), respectively.

In some cases, an estimation of the outage probability OP can be obtained on basis of only two parameters, the mean DGD $\langle\Delta\tau\rangle$ quantifying the PMD of the fiber link, and the maximum DGD value $\Delta\tau_{max}$ quantifying the system tolerance to a PMD distortion, respectively. $\Delta\tau_{max}$ is also referred to as the DGD tolerance of the system and denotes the DGD which leads to a BER of the threshold value used in the outage definition (e.g., 10^{-3}). Hence by neglecting the statistics of the PSP variation, the outage probability OP is the likelihood that the DGD $\Delta\tau$ exceeds $\Delta\tau_{max}$ and can be calculated by integrating the Maxwellian probability distribution $\rho(\Delta\tau)$ over $\Delta\tau > \Delta\tau_{max}$:

$$OP(\langle\Delta\tau\rangle) = \int_{\Delta\tau max}^{\infty} \rho(\tau)\, d\tau \qquad (2)$$

The integration shows that a system with a DGD tolerance of $\Delta\tau_{max}$ exhibits an OP of 10^{-5} at a PMD of $\langle\Delta\tau\rangle = \Delta\tau_{max}/3.2$.

However, this simple relation between outage probability and PMD of a link depends on two assumptions: first (1), that the first-order PMD model holds and, second (2), that the Maxwellian distribution ρ is also true for samples picked over time at a fixed wavelength and not only for DGD samples obtained from a wavelength scan.

1. A closer look at the validity of the first-order model revealed that DGD and PSP remain constant within the signal spectrum, if the product $\Delta\nu\,\langle\Delta\tau\rangle$ of spectral width and the PMD is sufficiently small. Practically, this is often the case for transmission systems with low chirp external modulators, without pulse carving for return-to-zero (RZ) modulation, and with only weak or without PMD mitigation. On the other hand, if the product is too large, the auto-correlation function of DGD and PSP [26] indicates decorrelation within the signal spectrum. Then the likelihood of second- and higher-order PMD distortions is no longer negligible. The second-order effects of PMD are polarization-dependent chromatic dispersion (PCD) and depolarization (DEP). They lead to additional distortions of the optical signal field [7, 31].
2. The validity of the Maxwellian distribution was investigated by the analysis of long-term measurement of installed fiber DGD [1, 2, 3]. It turned out that, in general, only DGD samples of a wavelength scan confirm the Maxwellian distribution ρ. On the other hand, the statistics of the DGD seen by a signal at a fixed wavelength is not always converging to ρ for installed fiber links. The difference between wavelength and time statistics can be explained by the "Hinge model" of PMD [2, 32].

Opposite to OP assessment based on the Maxwellian distribution (equation 2) where all wavelength channels have the same OP, in a fiber with Hinge behavior some wavelength channels might exhibit a higher and some a lower OP [32]. Even though the PMD tolerance assessment of modulation formats and mitigation schemes is commonly based on OP definition, which does not consider the Hinge model, this simplified approach remains an excellent tool to compare performances towards PMD.

Outage durations of hours have been deduced from PMD measurements of buried fiber similar to Figure 2. Nevertheless, in some cases PMD fluctuations on the time scale of a few milliseconds have been observed for aerial cables or fiber exposed to mechanical vibrations. If these fast fluctuations need to be compensated, they determine the upper speed limit of a PMDC.

The PMD of a fiber is often quantified by the PMD coefficient $\tau' = \langle\Delta\tau\rangle/\sqrt{L}$, which describes the growth of the mean DGD $\langle\Delta\tau\rangle$ with the fiber link length L. In order to assess the impact of PMD on a transmission system, the value of τ' needs to be related to the PMD tolerance (PMD_{tol}) and to L. Fiber PMD (PMD_{fiiber}) and all component and subsystem PMDs (PMD_i) contribute to the total link PMD_{tot} according to $PMD_{tot}^2 = PMD_{fiber}^2 + \Sigma PMD_i^2$. The maximum link length is $L \leq (PMD_{tol}^2 - \Sigma PMD_i^2)/\tau'^2$. With recently manufactured fiber having a low PMD coefficient of 0.08 ps/$\sqrt{}$km or less, and assuming a dispersion compensation fiber PMD coefficient of 0.15 ps/$\sqrt{}$km, an amplifier PMD of 0.5 ps, and 80 km amplifier spacing, 40 Gb/s transmission over long haul distances is affected by PMD beyond 1,400 km. In fiber production minor attention has been paid to PMD up to the mid-90s. Therefore, links incorporating older fibers might exhibit PMD coefficients of 0.5 ps/$\sqrt{}$km and beyond. This means that a link of a few hundred kilometers might reach the PMD limit, even at 10 Gb/s.

Optical PMDC

Optical PMDCs were the first approach that was proposed and demonstrated to combat PMD effects, and they are the most effective PMD compensation technique for the direct detection optical communication systems.

Operation Principle of Optical PMDC

Except the PSP launching, where a polarization controller (PC) is used at the transmitter to align the SOP of the signal with one of the PSPs of the link, an optical PMDC is designed to have PMD characteristics reverse to that in the transmission link [48]. In an optical fiber transmission system, PMD can be modeled as a concatenation of many birefringent elements. In principle, at the receiver side, if an optical PMDC consisting of as many birefringent elements as those in the transmission link can be set in such a way that the birefringent elements are opposite to the corresponding birefringent elements in the link, PMD can be completely compensated. However, it is not only impractical for an optical PMDC to have so many birefringent elements, but also hard to control them. In a real system, an optical PMDC has only been achieved up to second-order approximation, with a few birefringent elements.

Figure 3 shows the structure of a typical optical PMDC. It consists of an adaptive compensation element,

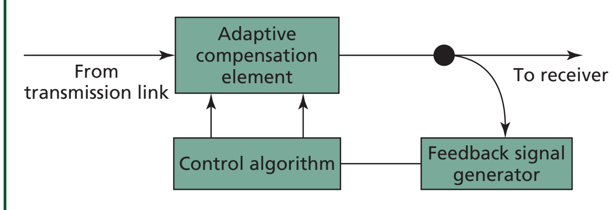

Figure 3.
Structure of an optical PMD compensator.

a feedback signal generator, and a control algorithm unit. The adaptive compensation element usually comprises a few PCs and birefringent elements. An optical PMDC is dynamically adjusted with a feedback signal to track the PMD and SOP variation in a real system. Widely used feedback signals for optical PMDCs are degree of polarization (DOP), radio frequency (RF) tones, RF power within a certain bandwidth, and eye-opening [9, 16, 44, 53]. The control algorithm works in a tracking mode to follow the PMD variation in the link by optimizing the feedback signal. Either trial-and-error or some gradient search algorithms can be used.

Effect of Modulation Format on Optical PMDC

Modulation formats affect optical PMDCs in three ways. First, they have an impact on the effectiveness of an optical PMDC; second, the lengths of birefringent elements in an optical PMDC are modulation format dependent; and third, the efficiency of some feedback signals depends on the modulation format.

PMD impairments depend on modulation formats. When there is no PMD compensation, PMD penalty is mainly caused by first-order PMD, and it induces a larger penalty on a modulation format with a wider pulse (narrower bandwidth). When there is PMD compensation, higher-order PMD effects become dominant, and a signal with a larger bandwidth (narrower pulse width) gets less improvement from the PMD compensation [54]. **Figure 4** shows performance of a single-stage optical PMDC with a variable birefringent element for NRZ, 33 percent duty-cycle return-to-zero, and 67 percent duty-cycle carrier-suppressed RZ (CSRZ) on-off keying (OOK) signals [54]. For comparison, the performance of the signals without any

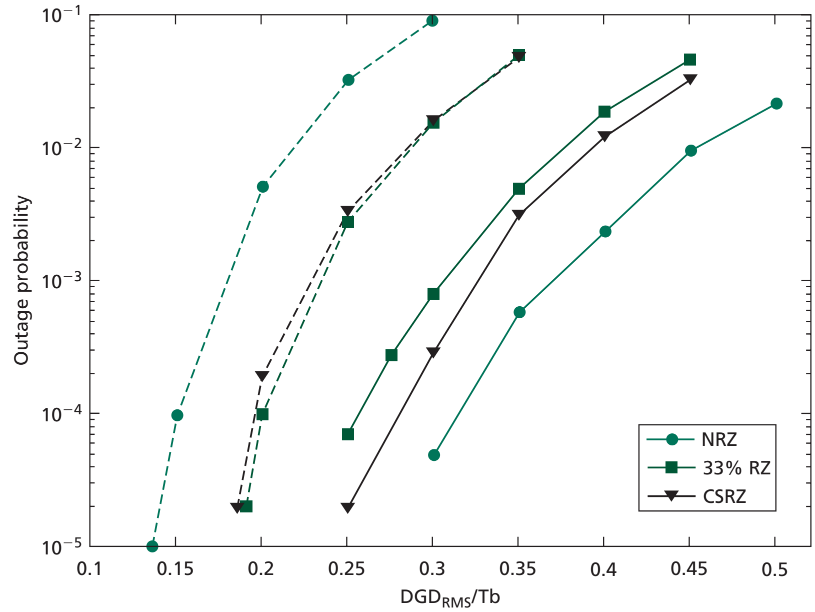

Figure 4.
Outage probability of a one-stage PMDC for different modulation formats.

PMD compensation is also given in the figure. The OP in the figure is defined for a BER = 10^{-12} with 1 dB OSNR margin. It shows that, at an OP of 10^{-4}, the optical PMDC can improve the PMD tolerance of NRZ-OOK by about two times but can only obtain about 25 percent improvement for the RZ-OOK. Based on this fact, the use of a narrow bandwidth filter before an optical PMDC has been proposed to increase the benefit of the optical PMDC for an RZ signal. Although the sensitivity of the system is reduced, the overall PMD tolerance of the system can be increased [39].

The purpose of an optical PMDC is to reduce the total PMD, but under some conditions, the optical PMDC can increase the total higher-order PMD. For example, the total second order PMD in a transmission link with an optical PMDC is

$$\vec{\Omega}_t' = R\vec{\Omega}_f' + \vec{\Omega}_c' + \vec{\Omega}_c \times \vec{\Omega}_t \qquad (3)$$

where $\vec{\Omega}_t$ is the overall PMD vector, $\vec{\Omega}_f$ and $\vec{\Omega}_c$ are PMD vectors of the transmission link and PMDC, respectively, and R is the rotation matrix of the PMDC. If only considering first-order PMD effects, an optical PMDC with a larger differential group delay can compensate more PMD. However, according to equation 3, an optical PMDC with a large DGD is more likely to increase the overall second-order PMD, which degrades the overall performance of the optical PMDC. Therefore, there is an optimum DGD value for the optical PMDC, which tends to be smaller for a modulation format with a larger bandwidth, as a signal with a larger bandwidth is more susceptible to higher-order PMD effects [51].

The efficiency of the feedback signal, DOP, also has a strong dependence on the modulation format. Only for NRZ and differential phase shift keying, the DOP is monotonic with DGD. For RZ-OOK and CSRZ,

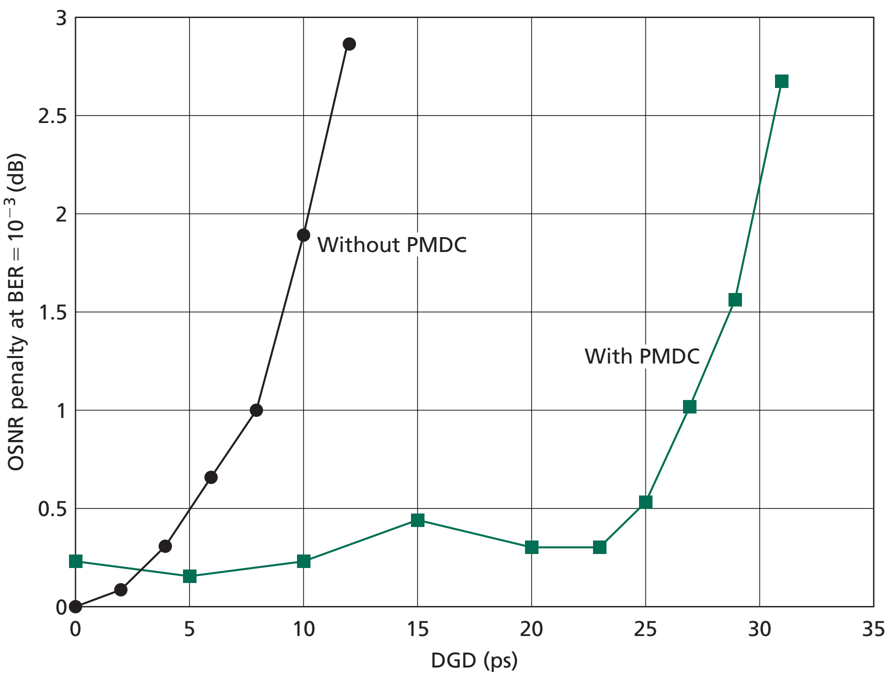

BER—Bit error ratio
dB—Decibel
DGD—Differential group delay
DPSK—Differential phase shift keying
NRZ—Non-return-to-zero
OSNR—Optical signal-to-noise ratio
PMD—Polarization mode dispersion
PMDC—PMD compensator
ps—Picosecond

Figure 5.
Performance of a two-stage optical PMDC for 42.8 Gb/s NRZ-DPSK.

the DOP oscillates with DGD. An RZ signal also has a smaller unambiguous DGD detection range than NRZ. These features of DOP will affect the performance of an optical PMDC. Therefore, DOP cannot be directly used as a PMDC feedback signal for all the modulation formats. For some modulation formats, a narrow bandwidth filter has to be used either to reduce the oscillation of the DOP with DGD or to increase the unambiguous DGD range [53].

Performance of Optical PMDC

Figure 5 shows the performance of an optical PMDC. It is a two-stage optical PMDC with one piece of polarization maintaining fiber (PMF) in each stage [50]. Lithium niobate ($LiNbO_3$) polarization controllers are used so it can track fast PMD and polarization variation. The measured OSNR penalty of a 42.8 Gb/s NRZ-DPSK with and without the optical PMDC is shown in Figure 5. In the measurement, a first-order PMD emulator was used, and one polarization scrambler (PS) was inserted in front of the PMD emulator to simulate the SOP changes and one PS after the PMD emulator to simulate the PSP changes. It shows that the optical PMDC can increases the PMD tolerance of the 42.8 Gb/s DPSK by a factor of three.

Electronic Distortion Equalizers

Electronic distortion equalizers (EDEs), often referred to as electronic dispersion compensators (EDCs), are adaptive electronic circuits which perform signal processing just after optical detection at the receiver side to remove part of the distortion due to transmission. Thanks to their integration as a simple electronic chip into an optical receiver board, they offer a promising and potentially low-cost alternative or complementary approach to adjustable optical means for reach and bit-rate upgrades [4, 6, 25, 40].

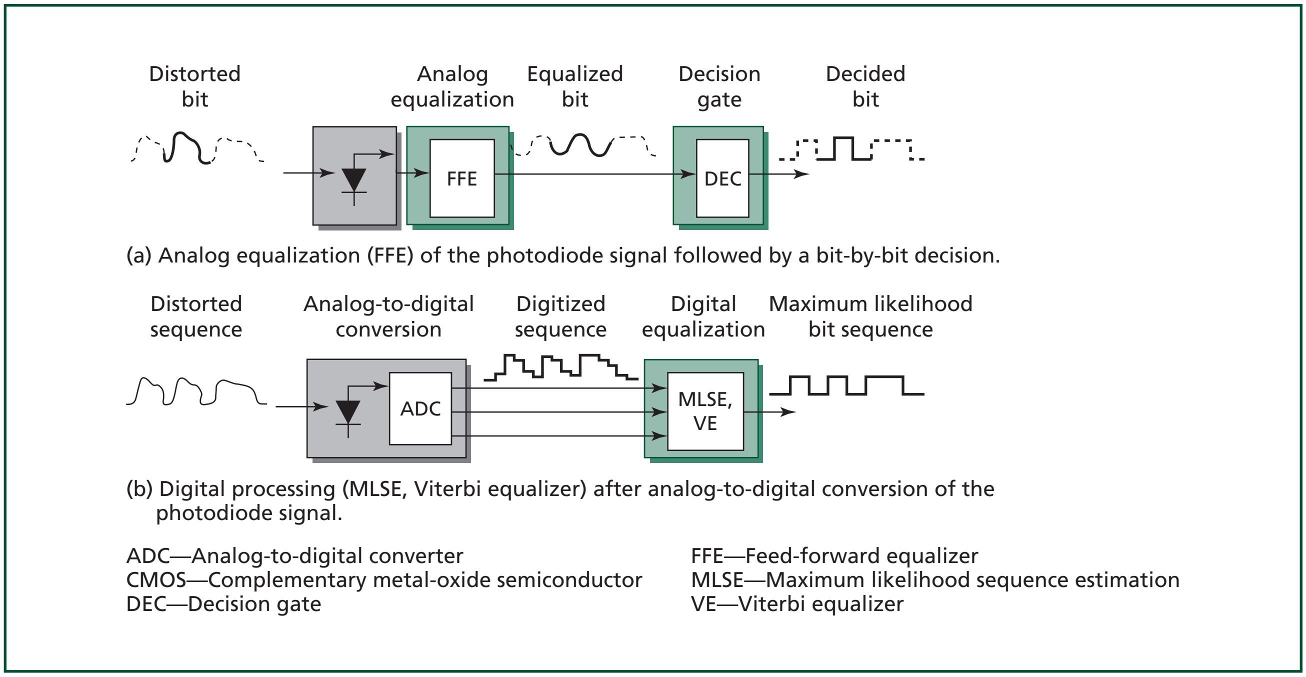

Figure 6.
Solutions for electronic distortion equalizers.

Optical methods like dispersion compensating fibers or optical PMD compensators can generally outperform an electrical equalizer. This is due to the loss of optical phase and polarization information after detection by a photodiode. Nevertheless, a single, low-cost EDE chip implemented in each receiver will potentially enable progress toward extended reach lengths, or toward higher bit rates. Moreover, it relaxes the design constraints on the optical infrastructure. In certain cases it can allow the removal of expensive, finely tuned optical distortion compensators inserted at the receiver side.

This section will introduce the basic principles of both analog and digital electronic distortion equalizer approaches and explain the potential transmission system enhancements and applications. Bell Labs realized and successfully tested an advanced EDE circuit for a high bit rate of 43 Gb/s [19, 20].

Two different basic types of electronic equalizers exist, using either analog or digital processing means. Both equalizer types can be realized as an application-specific integrated circuit (ASIC), on a chip area of a few square millimeters, and adapt automatically to any slowly varying distortion without the need for a training sequence. **Figure 6** displays the principal receiver architectures. **Figure 7** shows analog and digital signal processing circuits based on silicon germanium (SiGe) and complementary metal-oxide

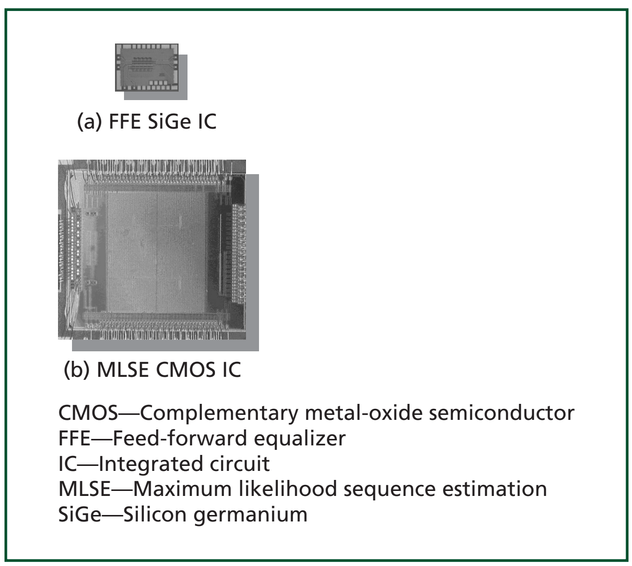

Figure 7.
Analog and digital signal processing circuits.

semiconductor (CMOS) electronic technology integrated circuits (ICs).

Analog Equalizers

Analog electronic equalizers include multi-tap feed-forward equalizers (FFE), decision feedback equalizers (DFE), and combinations of both. The DFE includes the decision gate. This type of equalizer processes several consecutive bits at the same time, but the data then will be decided bit-by-bit.

As mentioned previously, FFE and DFE have already been realized for 43 Gb/s in an advanced, state-of-the-art SiGe bipolar semiconductor technology with transit frequencies beyond 200 GHz. The 43 Gb/s FFE uses distributed electrical amplifiers serving as delay elements and adjustable analog four-quadrant multipliers, which allow the superimposition of weighted signal parts to realize the target filter function.

The analog four-quadrant multipliers, also referred to as taps, must be adapted automatically to allow for transmission over dynamically distorted fiber links. Different techniques are available for the automatic adaptation of analog electronic equalizers. In systems using FEC, the count of the corrected errors can be used as the feedback signal for the adaptation algorithm. The error count is applied in a dither algorithm for adaptation of the FFE and the decision circuit, where each tap and the decision threshold, respectively, are optimized independently to minimize the error count. Due to the random occurrence of bit errors, a sufficiently high number of errors must be evaluated in order to obtain a stable feedback signal. Since the transmission system is operated with margin at a worst case pre-FEC BER of $10^{-5} \ldots 10^{-4}$, update of the feedback signal can be expected within a few milliseconds (ms), resulting in a complete adaptation within some hundred ms.

An alternative method is to insert an eye monitor in parallel with the decision circuit. This eye monitor evaluates the vertical eye opening of the received data signal by measuring the mean and rms values of ones and zeros. Two versions are possible: The serial eye monitor consists of a decision circuit, where the threshold and sampling phase are continuously tuned. The parallel eye monitor uses an analog-to-digital converter (ADC). Both eye monitors provide a parameter that is related to the eye opening or the Q-factor of the eye diagram of the equalized signal. This parameter is then used in the same dither algorithm as with the error count feedback. Since the eye monitor works independently of the decision circuit, it enables a faster adaptation speed than obtained by using the FEC error count.

Digital Equalizers

Digital electronic equalizers use the maximum likelihood sequence estimation (MLSE) by implementation of the Viterbi algorithm. They require more complex signal processing compared with the analog equalizer. First, it converts the received data signal into digitized samples using an analog-to-digital converter with 3–4 bit resolution. Then it calculates the most probable received sequence in a digital processor using the Viterbi algorithm: i.e., it simultaneously processes and decides a data sequence resulting in a potentially higher performance compared to the analog type. The adaptation of the digital equalizer is done by a statistical analysis of the formerly received data signals, which are available within the digital equalizer. The adaptation speed is then comparable to that of the analog equalizer using the parallel eye monitor.

State-of-the-art realizations of Viterbi equalizers for 10 Gb/s receivers are based on a high-speed chip for analog-to-digital-converters in silicon germanium bipolar technology with up to 1000 transistors, and on a CMOS chip for digital processing with several hundred thousand transistors [14]. Recently, a complete 10 Gb/s MLSE has been realized on a single CMOS chip [21].

Performance of EDE

The PMD tolerance of high-speed optical transmission systems can be enhanced considerably by the use of EDEs. **Figure 8** shows the result of a theoretical analysis on the tolerance improvement provided by analog and digital EDEs, respectively, in comparison to systems with standard receivers at 10 Gb/s NRZ-OOK transmission. It must be noted here that it is easier in simulations as well as in experiments to determine the DGD tolerance rather than the PMD tolerance. As already mentioned in the section titled "Impact of PMD on Transmission," a fraction of 3.2

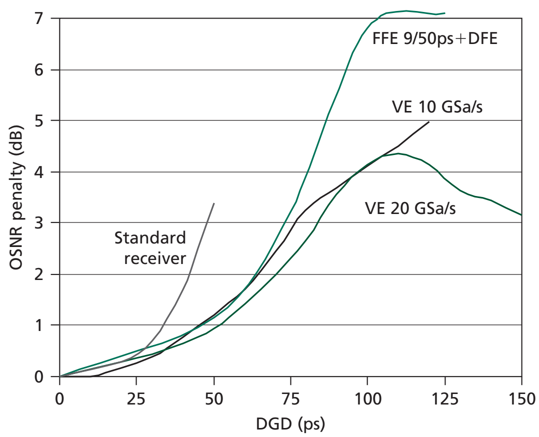

dB—Decibel
DFE—Decision-feedback equalizer
DGD—Differential group delay
FFE—Feed-forward equalizer
GSa/s—Gigasamples per second
OSNR—Optical signal-to-noise ratio
ps—Picosecond
VE—Viterbi equalizer

Figure 8.
Comparison of the DGD tolerance of a standard receiver with receivers with analog (FFE + DFE) or digital equalizers (Viterbi equalizer) at 10 Gb/s.

of the DGD tolerance value is equivalent to the mean PMD that produces the same penalty at an OP of 10^{-5}. Although higher-order PMD is neglected, the improvement of the DGD tolerance by electronic equalization is roughly comparable to that seen in the all-order PMD tolerance.

A 40 percent increase in DGD tolerance is observed for the analog and the digital equalizer at 1 dB OSNR penalty. The superior performance of the digital equalizer becomes obvious at OSNR penalties higher than about 2 dB. Especially, if the incoming data is two times oversampled with 20 Gigasamples per second (GSa/s) the digital equalizer allows for DGD higher than one bit period at a maximum OSNR penalty of about 4.5 dB.

Extensive experiments explore the system improvements enabled by analog equalizers. An adaptive 43 Gb/s receiver has been experimentally evaluated applying different modulation formats: NRZ/RZ-OOK and NRZ/RZ-DPSK, and phase-shifted binary transmission (PSBT) [17]. The error count from an FEC unit has been used as feedback signal to adapt a 5-tap

Table I. Experimentally evaluated DGD tolerances of a 43 Gb/s adaptive receiver for various modulation formats.

Modulation format	DGD tolerance
OOK NRZ	10.8 ps (+70%)
OOK RZ	11.8 ps (+10%)
DPSK NRZ	10.5 ps (+60%)
DPSK RZ	12.0 ps (+15%)
PSBT	8.5 ps (+10%)

DGD—Differential group delay
DPSK—Differential phase shift keying
NRZ—Non-return-to-zero
OOK—On-off keying
ps—Picosecond
PSBT—Phase-shifted binary transmission
RZ—Return-to-zero

FFE and 1-tap DFE. **Table I** summarizes the achieved DGD tolerances for 1 dB OSNR penalty. The values in parentheses indicate the improvement compared to a standard receiver.

The higher improvements compared to those obtained by simulation for OOK-NRZ can be attributed to the mitigation of additional optical and electrical distortions of the system using the standard receiver.

Another experiment confirms the improvements in the tolerance against first- and-second order PMD for NRZ- and RZ-DPSK modulation formats by analog equalization. **Table II** summarizes the PMD tolerances of standard and adaptive receivers. In general, for an outage probability of 10^{-5}, the tolerances to first- and-second order PMD increase by 55 percent to 4.3 ps (NRZ) and 5.4 ps (RZ), respectively.

In high-speed systems based on symbol rates above 10 Gbaud, where PMD is a major impairment, the application of EDE will result in improved system performance. Even though optical PMDC may be required, depending on the available margins, EDE can relax their accuracy for transmission impairment compensation. Hence, per channel optical dispersion compensation could be avoided, and costly tunable optical compensators for each channel might be avoided in system environments with moderate PMD. For the case of low acceptable OSNR penalties, e.g.,

Table II. PMD for OP of 10^{-5} at 2 dB OSNR penalty.

PMD	DPSK-NRZ	DPSK-RZ
Standard RX	2.8 ps	3.5 ps
Adaptive RX	4.3 ps (+50%)	5.4 ps (+50%)

dB—Decibel
DPSK—Differential phase shift keying
NRZ—Non-return-to-zero
OP—Outage probability
OSNR—Optical signal-to-noise ratio
PMD—Polarization mode dispersion
ps—Picosecond
RX—Receiver
RZ—Return-to-zero

below 1 dB, analog and digital equalizers provide comparable PMD tolerances.

EDE is not restricted to a certain distortion, e.g., PMD, but can also be used to compensate for a multitude of distortions resulting in ISI, e.g., bandwidth limitations. Recent experiments explore the application of EDE in metro networks with limited optical bandwidths, e.g., in systems with 50 GHz granularity [18]. Furthermore, EDE and its adaptive and continuous adjustment can also compensate for long-term component drifts and aging, which could become a key advantage for systems using components at their physical limits.

PMD Compensation by Fast Polarization Scrambling

In this section we will first describe the principle of PMD mitigation by fast polarization scrambling. Then we will present the experimental setup and discuss some experimental results obtained in lab experiments at 43 Gb/s to verify this concept with segments with fixed DGD. The results obtained may not be directly applied to practical systems where the DGD of each section is varying with time and wavelength. A system with polarization scramblers can perform better or worse than a system without PSs at a given instance. For example, a link with a certain DGD can, at a given moment, consist of two sections whose DGD values add up to be equal, slightly larger, or much larger than the overall DGD value. If a PS is inserted between the two sections, the system performance in the first two cases will be better, but worse in the third case. The overall performance of a system depends the overall DGD value and the number of PSs used.

Principle of PMD Mitigation by Fast Polarization Scrambling

PMD mitigation by fast polarization scrambling was demonstrated using scrambling at the transmitter [49] and evaluated by simulation for distributed scrambling [8, 13, 36, 52]. **Figure 9** illustrates principles of PMD compensation by scrambling. The basic

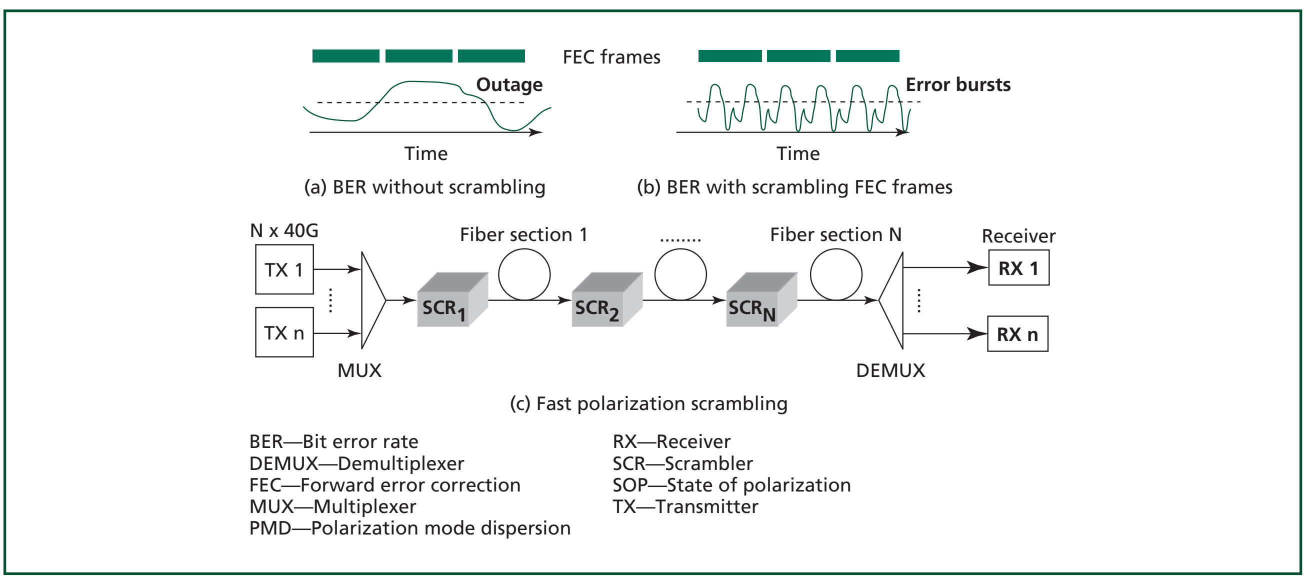

Figure 9.
Principles of PMD compensation.

principle of these schemes, as shown in Figure 9a and Figure 9b, is that the scramblers accelerate the PMD statistics of the transmission fiber down to sub-FEC frame duration (e.g., 12 μs for OTU-2 FEC). Hence PMD-induced outage times are transformed to short error bursts, as shown in Figure 9b, and can be corrected by the FEC. This approach has the charm of being inherently dense wavelength division multiplexing (DWDM) capable, as the polarization scramblers are located in the fiber link and PMD mitigation is achieved for all DWDM channels simultaneously.

Figure 9c displays a typical setup for fast polarization scrambling for N×40 Gb/s. The fast polarization scramblers SCR_1 to SCR_n are located along the whole fiber link: the first scrambler in front of the first fiber section, and the next scramblers after each fiber section. In principle, each fiber section can be of different length, depending on the PMD of this section.

Experimental Setup

A similar setup to that shown in Figure 9c was also used for experiments in the laboratory by using five scramblers and four sections of 80 km single mode fiber (SMF). Each section was loaded with additional PMD by DGD emulators and/or PMF fibers with fixed lengths (e.g., 3.44 ps, 3.44 ps, 3.0 ps, and 2.5 ps) to emulate the transmission over a fiber link with slowly drifting PMD. In front of each tunable DGD-emulator, a slow mechanical scrambler was used to ensure worst-case measurements of PMD effects.

Each polarization scrambler consisted of a polarization modulator with several segments acting, for example, as quarter waveplates and RF electronics to modulate the segments by sinusoidal driving voltages of certain frequencies. For the experiments, a $LiNbO_3$ polarization modulator with three sections of three differently oriented waveplates was used. The retardation of the waveplates is modulated via three electrodes. They are driven at slightly different frequencies of f, $f + 0.2$ MHz, and $f + 0.4$ MHz ($f = 5 \ldots 50$ MHz). The difference frequency depends on the FEC used, as it should be faster than the FEC frame rate (approximately 100 kHz for a FEC operating at 10 Gb/s).

For the 40 Gb/s experiments an enhanced or ultra FEC (UFEC) operating at 10 Gb/s as well as commercially available UFECs operating at 40 Gb/s were used. In case of the 10 Gb/s FEC, the data signal of one of the four 10-Gb/s tributaries is obtained by FEC encoding and decoding of a $2^{23}-1$ pseudo random bit sequence (PRBS) sequence (UFEC with net coding gain of 8.6 dB). The other three 10.7 Gb/s tributaries are loaded with $2^{23}-1$ PRBS sequence. All four tributaries were then multiplexed to the 43 Gb/s data sequence.

The receiver comprises a 1 bit delay interferometer to demodulate the DPSK signal and a balanced detector in front of a Serdes Framer Interface Level 5 (SFI-5) deserializer chip. The four tributaries at the deserializer outputs, which belong to the 10.7 Gb/s FEC channel, were multiplexed and launched into the FEC decoder. Pre-FEC and post-FEC BER were measured by bit-error-rate detectors. The measurements at post-FEC BER were generally performed over several minutes and some samples (at the 1 dB limit) were also measured over longer periods (up to two hours) to ensure no occurrence of uncorrectable error bursts.

In case of the 40 Gb/s UFEC, commercial transponders were used and the pre- and post-FEC error count was directly read out from the FEC chip by software.

Receiver OSNR was varied by an attenuator and OSNR penalty was generally measured with respect to back-to-back measurements.

Experimental Results and Discussion

By using a set of four PMF fibers of 3.44 ps, 3.44 ps, 3 ps, and 2.5 ps and varying the DGD emulator after the first scrambler between 0 and 12 ps, the OSNR penalty versus mean DGD (mean DGD = $\sqrt{(DGD_1^2 + \ldots + DGD_5^2)}$) was measured. **Figure 10** displays mean DGD tolerance versus OSNR penalty for two different scrambler frequencies of 5 MHz (black squares) and 50 MHz (gray triangles) for NRZ-DPSK at the post-FEC BER of 10^{-9} [29].

In order (1)to confirm that no error bursts which cannot be handled by the FEC are present and (2) to determine the additional improvement which might be attributed to the FEC's burst error correction capability at a high scrambling speed [19] of 5 MHz or 50 MHz, the DGD tolerance was measured by observing the post FEC BER (FEC-BER) and keeping it at 10^{-9}. It was shown in [29] that the mean DGD tolerance for a

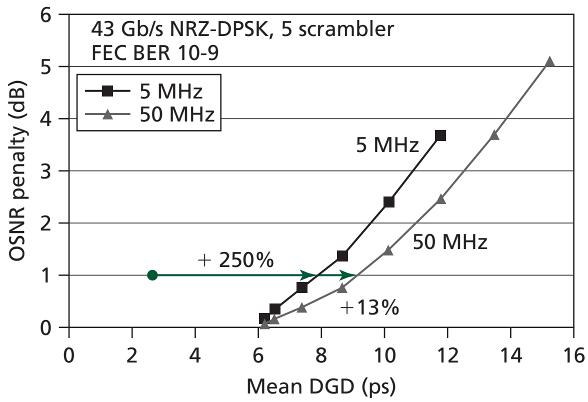

BER—Bit error ratio
dB—Decibel
DGD—Differential group delay
DPSK—Differential phase shift keying
FEC—Forward error correction
NRZ—Non-return-to-zero
OSNR—Optical signal-to-noise ratio
ps—Picosecond

Figure 10.
OSNR penalty versus mean DGD for 43 Gb/s NRZ-DPSK for 5 polarization scramblers with 5 and 50 MHz scrambling frequency at a BER after FEC of 10^{-9}.

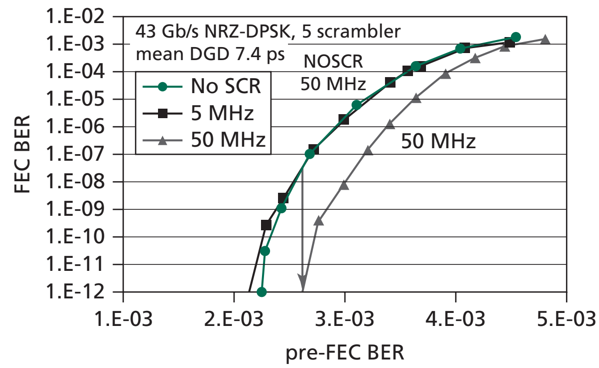

BER—Bit error ratio
DGD—Differential group delay
DPSK—Differential phase shift keying
FEC—Forward error correction
NRZ—Non-return-to-zero
ps—Picosecond
SCR—Scrambler

Figure 11.
Comparison of FEC BER versus pre-FEC BER for 43 Gb/s NRZ-DPSK with no polarization scramblers and with polarization scramblers at 5 and 50 MHz, respectively.

small number of polarization-maintaining sections provides an upper limit and converges to the fiber PMD tolerance for an increasing number of PM sections.

Scrambling at 5 MHz leads to an improvement in DGD tolerance at a 1 dB OSNR penalty of 250 percent to 7.6 ps (compared to the case with scramblers off). A further improvement of 13 percent is observed by the use of a higher scrambling frequency, e.g., 50 MHz, leading to a mean DGD tolerance of 9.2 ps (NRZ-DPSK), which corresponds to 40 percent of the bit period. A change of the modulation format to RZ-DPSK resulted in similar observations [27] leading to a mean DGD tolerance of 10.2 ps and 11.8 ps (47 percent of the bit period) at low (5 MHz) and fast (50 MHz) scrambling speed, respectively. (RZ modulation formats show inherently a higher tolerance to DGD than NRZ formats; see, for example, [22]). This moderate additional improvement of less than 20 percent underlines the explanation that if the scrambling period is faster than the FEC frame duration the dominant effect is a randomization of the errors by scrambling and FEC interleaver [27].

In order to investigate whether or not the FEC burst-error correction capability enhances the mean-DGD tolerance, **Figure 11** plots the FEC output BER (denoted FEC-BER, y-axis) versus input BER (denoted pre-FEC BER, x-axis) at different scrambling frequencies of 5 and 50 MHz and without scramblers (corresponding to a mean DGD of 0 ps).

The set of 5 DGDs had a mean DGD of 7.4 ps when scramblers were present. At scrambling frequencies of 50 MHz (gray triangles), an improvement is observed as compared to the 5-MHz curve (black boxes), which is nearly identical with the FEC-performance without scrambling (mean DGD 0 ps, green dots). At 50 MHz scrambling frequencies, a higher pre-FEC error rate can be corrected by the FEC than for a 5 MHz scrambling frequency. This behavior is attributed to the FEC burst error correction capability, which maps to the additional 13 percent improvement in mean DGD tolerance shown in Figure 10. This has also been observed in the 10 Gb/s experiment reported in [35].

These single-channel results were also confirmed in a DWDM experiment with scrambling of 42 channels simultaneously [28], demonstrating the DWDM capability of this PMD mitigation technique. Finally a comparison of different 40 Gb/s FECs was performed [30], which demonstrated the different burst-error correction capabilities of the commercially available 40 Gb/s FECs.

To link the PMD tolerance in systems with fixed DGD sections to that with time-varying DGD sections, a scaling rule was proposed in [52]:

$$\langle DGD \rangle_{\text{variedDGDs}} = \langle DGD \rangle_{\text{fixedDGDs}} / x \qquad (4)$$

where the factor x depends on the number of PSs N and OP. For N = 1 and an OP of 10^{-5}, it is well known that the factor x is about 3, assuming the Maxwellian distribution of DGD. For N > 1, x is between 3 and 1 and can be empirically obtained through numerical simulations. The outage probability improves with N and depends on the distribution of the PSs among the total link PMD. A PMD tolerance of 5.5 ps can be expected for an outage probability of 10^{-5} and 5 PSs for a 40 Gb/s NRZ-DPSK system assuming that the PMD is distributed uniformly among the scrambler sections.

DSP-Enabled PMDC Techniques

With the advances in high-speed digital signal processing (DSP) and analog-to-digital converter circuits, powerful digital PMDC techniques have recently emerged. The first digital PMDC technique is based on digital coherent detection [15, 23, 33, 38, 43, 45]. The second is based on coherent optical OFDM (CO-OFDM) [24, 34, 37, 46, 47]. In this section, we will briefly discuss both techniques.

Digital PMDC in Digital Coherent Receiver

Due to the progress in high-speed electronic DSP, there has been revived interest in optical coherent detection. Polarization division multiplexed QPSK (PDM-QPSK) with coherent detection has been proposed as one of the solutions to upgrade the existing 10 Gb/s wavelength division multiplexing networks with 50 GHz channel spacing to 40 Gb/s or 100 Gb/s [23, 33, 38, 45]. Digital coherent detection, where the full optical field information is accessible, has the potential to increase the spectral efficiency with multi-level modulation and to compensate all linear transmission impairments such as chromatic dispersion (CD) and polarization mode dispersion in the electrical domain by DSP. **Figure 12** is the block diagram of a typical intradyne digital coherent receiver. After passing through a polarization beam splitter (PBS), each polarization of the received signal is combined with a local oscillator (LO) in a 90° hybrid. After the hybrids, the four tributaries of the signal are detected by four detectors, then sampled and digitalized for further processing. The DSP is usually composed of four steps:

1. CD compensation,
2. Polarization demultiplexing and equalization,
3. Carrier phase estimation, and
4. Symbol identification.

The polarization demultiplexing and equalization are achieved with four parallel electronic equalizers. Assuming that the transfer functions of the four equalizers are h_{xx}, h_{xy}, h_{yx}, and h_{yy}, respectively, the

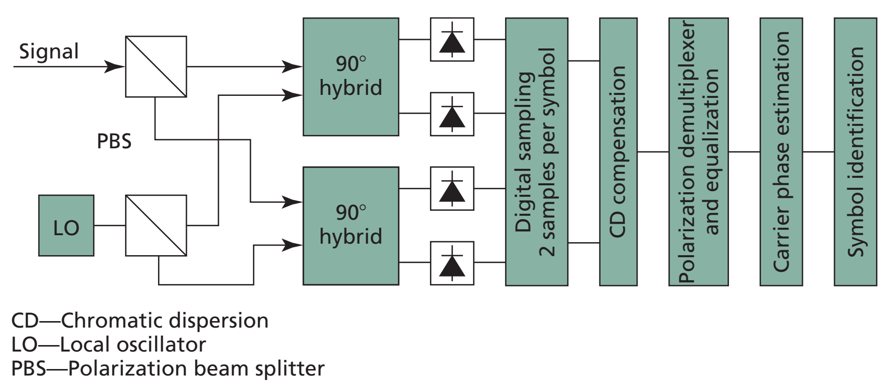

Figure 12.
Schematic of digital coherent detection for a polarization-division-multiplexed signal.

input and output signals of the equalizers can be expressed as

$$\begin{pmatrix} E'_x \\ E'_y \end{pmatrix} = \begin{pmatrix} h_{xx} & h_{xy} \\ h_{yx} & h_{yy} \end{pmatrix} \begin{pmatrix} E_x \\ E_y \end{pmatrix} \quad (5)$$

In principle, if the Jones matrix $H = \begin{pmatrix} h_{xx} & h_{xy} \\ h_{yx} & h_{yy} \end{pmatrix}$ is inverse to the Jones matrix of the transmission link, the PMD effects can be completely compensated.

The equalizers can be realized with fractional spaced equalizers (FSEs). Intuitively, to compensate a DGD of τ, the number of taps the FSEs require is [23]

$$N = \tau M / T_s \quad (6)$$

where M is the number of samples per symbol, and T_s is the symbol period. In a real system, to perform polarization demultiplexing and PMD compensation, a blind equalization algorithm is required, for example, the constant-modulus algorithm [45]. Due to the existence of higher-order PMD and the use of blind equalization, a larger number of taps than that equation 6 is usually needed.

Digital PMDC in CO-OFDM

OFDM is a widely used modulation/multiplexing scheme in wireless and has recently been introduced to optical fiber communications [37, 46]. Optical OFDM, together with digital coherent detection, potentially allows for simple compensation of linear fiber transmission impairments such as PMD. In combination with PDM, high-speed CO-OFDM transmissions with high PMD tolerance have recently been demonstrated [24, 47].

In PDM-OFDM, the original data are first divided into x- and y-polarization branches, each of which is mapped onto many frequency subcarriers with certain modulation, which, together with pilot subcarriers, are transferred to the time domain by inverse Fourier transformation. The cyclic prefix is then used to accommodate inter-symbol interference caused by effects such as dispersion and PMD. The time-domain samples are converted by two digital-to-analog converters before driving two in-phase/quadrature (I/Q) modulators. The modulated optical signals are combined by a polarization beam splitter for PDM. Training symbols (TSs) are inserted into the symbol sequence to simplify channel estimation. At the receiver, digital coherent detection with polarization diversity is used to sample the fields of two orthogonal components of the received optical signal. Symbol synchronization is then performed [24, 47], and TSs are extracted for channel estimation. Detailed descriptions on the channel estimation and compensation method for PMD have been given in various previous papers [5, 24, 34, 47]. The PMD tolerance of a 112 Gb/s PDM-OFDM signal was shown to be larger than 100 ps (in terms of <DGD>) even when high-order PMD effects were taken into consideration [5, 34]. For a more detailed discussion on CO-OFDM we refer to the paper "Optical OFDM: A Promising High-Speed Optical Transport Technology," in this issue [5].

Conclusion

In **Table III**, we give an overview of the PMD tolerance of the different mitigation schemes discussed so far and relate them to the additional technical effort required for realization. In Table III the bit rate was chosen to be 40 Gb/s. Starting with the second row in Table III, we find the standard receivers for binary NRZ–OOK modulation exhibiting a PMD tolerance in the range of nearly 3 ps. This value serves as the reference for the improvement of the mitigation schemes. The analog (FFE, DFE) or digital (MLSE) electronic equalizers improve the PMD tolerance to 4.3 ps and 4.8 ps, respectively, with a moderate effort of less than 1,000 transistors for analog signal processing, or a higher technical effort, a fast ADC, and a DSP chip with a few million gates for the MLSE. The MLSE outperforms the analog equalizer provided the system tolerates a higher penalty (5 dB instead of 2 dB).

Optical processing of the received signal fields within a two-stage PMD compensator increases the PMD tolerance to roughly 9 ps. For a dynamic compensator, two fast polarization controllers, mostly manufactured as an integrated-optic structure in a lithium niobate crystal, and drive electronics for the electrodes need to be added to the receiver board.

On one hand, the realization of coherent PDM-QPSK or OFDM (last three rows in Table III) means a very high technical effort within the line cards, i.e., four or two fast ADCs, very high gate-count DSP chips (beyond ≈20 Mio gates), but, on the other hand,

Table III. Comparison among different PMD mitigation schemes for 40 Gb/s transmission (2 dB OSNR penalty, 10^{-5} outage probability, NRZ, except for coherent optical OFDM).

Mitigation scheme	PMD tolerance	Complexity per channel
Standard receiver	2.8 ps	–
Analog electronic equalizer	4.3 ps	<1000 transistors
Digital MLSE	4.8 ps	1 ADC + ≈5 Mio CMOS gates
Optical PMD compensator (2 stages)	9 ps	2 el.-opt. pol. modulators + monitoring/control unit
Distributed scrambling	5.5 ps	≥5 el.-opt. pol. modulators shared by all WDM channels
Coherent optical OFDM	100 ps	4 DACs, 4 ADCs + ≈20 Mgates
Coherent PDM-QPSK	30 ps	4 ADCs + ≈20 Mgates

ADC—Analog-to-digital converter
CMOS—Complementary metal-oxide semiconductor
DAC—Digital-to-analog converter
dB—Decibel
MLSE—Maximum likelihood sequence estimation
NRZ—Non-return-to-zero
OFDM—Orthogonal frequency division multiplexing
OSNR—Optical signal-to-noise ratio
PDM—Polarization division multiplexed
PMD—Polarization mode dispersion
ps—Picosecond
QPSK—Quadrature phase shift keying
WDM—Wavelength division multiplexing

record PMD tolerances of about 30 ps or even more than 100 ps, respectively, can be achieved.

For the application in a high channel count WDM system, distributed polarization scrambling can be implemented with the least effort of all schemes, since the polarization modulators serving as polarization scramblers act on all channels simultaneously. However, simulations indicate that the PMD tolerance of this scheme is limited to less than about 6 ps and the performance depends on the distribution of the PMD along the link.

References

[1] C. Antonelli and A. Mecozzi, "Theoretical Characterization and System Impact of the Hinge Model of PMD," J. Lightwave Technol., 24:11 (2006), 4064–4074.

[2] M. Boroditsky, M. Brodsky, N. J. Frigo, P. Magill, C. Antonelli, and A. Mecozzi, "Outage Probabilities for Fiber Routes With Finite Number of Degrees of Freedom," IEEE Photonics Technol. Lett., 17:2 (2005), 345–347.

[3] M. Brodsky, N. J. Frigo, M. Boroditsky, and M. Tur, "Polarization Mode Dispersion of Installed Fibers," J. Lightwave Technol., 24:12 (2006), 4584–4599.

[4] F. Buchali and H. Bülow, "Adaptive PMD Compensation by Electrical and Optical Techniques," J. Lightwave Technol., 22:4 (2004), 1116–1126.

[5] F. Buchali, R. Dischler, and X. Liu, "Optical OFDM: A Promising High-Speed Optical Transport Technology," Bell Labs Tech. J., 14:1 (2009), 127–148.

[6] F. Buchali, G. Thielecke, and H. Bülow, "Viterbi Equalizer for Mitigation of Distortions From Chromatic Dispersion and PMD at 10 Gb/s," Proc. Optical Fiber Commun. Conf. (OFC '04) (Los Angeles, CA, 2004), vol. 1, paper MF85.

[7] H. Bülow, "System Outage Probability Due to First- and Second-Order PMD," IEEE Photonics Technol. Lett., 10:5 (1998), 696–698.

[8] H. Bülow, "Outage vs PMD Tolerance Trade-Off for Fast Polarization Scrambling," Proc. 32nd Eur. Conf. on Optical Commun. (ECOC '06) (Cannes, Fr., 2006), paper Th2.5.2.

[9] H. Bülow, W. Baumert, F. Buchali, and W. Kuebart, "Adaptation of an Electronic PMD Mitigator by Maximization of the Eye Opening," Proc. 26th Eur. Conf. on Optical Commun. (ECOC '00) (Munich, Ger., 2000), vol. 3, pp. 209–210.

[10] H. Bülow, F. Buchali, and A. Klekamp, "Electronic Dispersion Compensation," J. Lightwave Technol., 26:1 (2008), 158–167.

[11] H. Bülow and S. Lanne, "PMD Compensation Techniques," Polarization Mode Dispersion (A. Galtarossa and C. R. Menyuk, eds.), Springer, New York, 2005, pp. 225–245.

[12] H. Bülow and G. Veith, "Temporal Dynamics of Error-Rate Degradation Induced by Polarisation Mode Dispersion Fluctuation of a Field Fiber Link," Proc. 11th Internat. Conf. on Integrated Optics and Optical Fibre Commun. and 23rd

Eur. Conf. on Optical Commun. (IOOC-ECOC '97) (Edinburgh, Scot., 1997), vol. 1, paper MO3C, pp. 115–118.

[13] C. R. Davidson, H. Zhang, Y. Cai, L. Liu, J.-X. Cai, A. Pilipetskii, M. Nissov, and N. S. Bergano, "Direct Measure of System Margin Enhancement by Polarization Scrambling," Proc. Optical Fiber Commun. Conf. (OFC '04) (Los Angeles, CA, 2004), vol. 1, paper WE1.

[14] A. Färbert, S. Langenbach, N. Stojanovic, C. Dorschk, T. Kupfer, C. Schulien, J. P. Elbers, H. Wernz, H. Griesser, and C. Glingener, "Performance of a 10.7 Gb/s Receiver With Digital Equaliser Using Maximum Likelihood Sequence Estimation," Proc. 30th Eur. Conf. on Optical Commun. (ECOC '04) (Stockholm, Swed., 2004), paper Th4.1.5.

[15] C. R. S. Fludger, T. Duthel, D. van den Borne, C. Schulien, E.-D. Schmidt, T. Wuth, J. Geyer, E. De Man, Khoe Giok-Djan, and H. de Waardt, "Coherent Equalization and POLMUX-RZ-DQPSK for Robust 100-GE Transmission," J. Lightwave Technol., 26:1 (2008), 64–72.

[16] C. Francia, F. Bruyère, J.-P. Thiéry, and D. Penninckx, "Simple Dynamic Polarisation Mode Dispersion Compensator," Electronics Lett., 35:5 (1999), 414–415.

[17] B. Franz, A. Klekamp, D. Rösener, F. Buchali, and H. Bülow, "Performance Improvements of Different Modulation Formats by Applying Adaptive Electronic Equalisation in 43 Gbit/s Systems," Proc. 33rd Eur. Conf. on Optical Commun. (ECOC '07) (Berlin, Ger., 2007), paper Tu3.1.2.

[18] B. Franz, A. Klekamp, D. Rösener, F. Buchali, W. Kuebart, and H. Bülow, "Optical Channel Bandwidth Reduction Enabled by Electronic Equalization in 43 Gb/s Systems," Proc. Optical Fiber Commun./National Fiber Optic Engineers Conf. (OFC/NFOEC '08) (San Diego, CA, 2008), paper OTh06.

[19] B. Franz, D. Rösener, F. Buchali, H. Bülow, and G. Veith, "Adaptive Electronic Feed-Forward Equaliser and Decision Feedback Equaliser for the Mitigation of Chromatic Dispersion and PMD in 43 Gbit/s Optical Transmission Systems," Proc. 32nd Eur. Conf. on Optical Commun. (ECOC '06) (Cannes, Fr., 2006), paper We1.5.1.

[20] B. Franz, D. Rösener, R. Dischler, F. Buchali, B. Junginger, T. F. Meister, and K. Aufinger, "43 Gbit/s SiGe Based Electronic Equalizer for PMD and Chromatic Dispersion Mitigation," Proc. 31st Eur. Conf. on Optical Commun. (ECOC '05) (Glasgow, Scot., 2005), vol. 3, paper We1.3.1, pp. 333–334.

[21] R. A. Griffin, N. Swenson, D. Crivelli, H. Carrer, M. Hueda, P. Voois, O. Agazzi, and F. Donadio, "Combination of InP MZM Transmitter and Monolithic CMOS 8-State MLSE Receiver for Dispersion Tolerant 10 Gb/s Transmission," Proc. Optical Fiber Commun./National Fiber Optic Engineers Conf. (OFC/NFOEC '08) (San Diego, CA, 2008), paper OThO2.

[22] W. Idler, A. Klekamp, R. Dischler, J. Lazaro, and A. Konczykowska, "System Performance and Tolerances of 43Gb/s ASK and DPSK Modulation Formats," Proc. 29th Eur. Conf. on Optical Commun. (ECOC '03) (Rimini, It., 2003), paper Th2.6.3.

[23] E. Ip and J. M. Kahn, "Digital Equalization of Chromatic Dispersion and Polarization Mode Dispersion," J. Lightwave Technol., 25:8 (2007), 2033–2043.

[24] S. L. Jansen, I. Morita, T. C. W. Schenk, and H. Tanaka, "Long-Haul Transmission of 16×52.5 Gbits/s Polarization-Division-Multiplexed OFDM Enabled by MIMO Processing (Invited)," J. Optical Networking, 7:2 (2008), 173–182.

[25] H. Jiang, R. Saunders, and S. Colaco, "SiGe Equalizer IC for PMD Mitigation and Signal Optimization of 40 Gbits/s Transmission," Proc. Optical Fiber Commun. Conf. (OFC '05) (Anaheim, CA, 2005), vol. 3, paper OWO2.

[26] M. Karlsson, J. Brentel, and P. A. Andrekson, "Long-Term Measurement of PMD and Polarization Drift in Installed Fibers," J. Lightwave Technol., 18:7 (2000), 941–951.

[27] A. Klekamp and H. Bülow, "Record PMD Mitigation of 11ps for 43Gb/s RZ-DPSK by Distributed Polarisation Scrambling," Proc. 12th OptoElectronics and Commun. Conf. (OECC '07) (Yokohama, Japan, 2007), paper 13B4-5.

[28] A. Klekamp, S. Dupont, P. Plantady, G. Charlet, and H. Bülow, "PMD Mitigation for 42 × 43 Gb/s DPSK (NRZ and RZ) by Distributed Polarisation Scrambling Over 4820 km Long NZDSF Fibre," Proc. 33rd Eur. Conf. on Optical Commun. (ECOC '07) (Berlin, Ger., 2007), paper WeP082.

[29] A. Klekamp, B. Junginger, and H. Bülow, "Experimental PMD Mitigation for 43 Gb/s DPSK by Distributed Polarisation Scrambling Over 4 Spans SMF Fibre," Proc. 32nd Eur. Conf.

on Optical Commun. (ECOC '06) (Cannes, Fr., 2006), paper Th4.3.6.
[30] A. Klekamp, D. Werner, and H. Bülow, "Study of Different 40 Gbit/s FECs Regarding PMD Mitigation Efficiency by Fast Polarization Scrambling," Proc. Optical Fiber Commun./National Fiber Optic Engineers Conf. (OFC/NFOEC '08) (San Diego, CA, 2008), paper JWA54.
[31] H. Kogelnik, L. E. Nelson, J. P. Gordon, and R. M. Jopson, "Jones Matrix for Second-Order Polarization Mode Dispersion," Optics Lett., 25:1 (2000), 19–21.
[32] H. Kogelnik, P. J. Winzer, L. E. Nelson, R. M. Jopson, M. Boroditsky, and M. Brodsky, "First-Order PMD Outage for the Hinge Model," IEEE Photonics Technol. Lett., 17:6 (2005), 1208–1210.
[33] C. Laperle, B. Villeneuve, Z. Zhang, D. McGhan, H. Sun, and M. O'Sullivan, "Wavelength Division Multiplexing (WDM) and Polarization Mode Dispersion (PMD) Performance of a Coherent 40Gbit/s Dual-Polarization Quadrature Phase Shift Keying (DP-QPSK) Transceiver," Proc. Optical Fiber Commun./National Fiber Optic Engineers Conf. (OFC/NFOEC '07) (Anaheim, CA, 2007), paper PDP16.
[34] X. Liu and F. Buchali, "Improved Nonlinear Tolerance of 112-Gb/s PDM-OFDM in Dispersion-Uncompensated Transmission With Efficient Channel Estimation," Proc. 34th Eur. Conf. on Optical Commun. (ECOC '08) (Brussels, Belg., 2008), paper Mo.3.E.2.
[35] X. Liu, C. R. Giles, X. Wei, Y.-H. Kao, C. Xie, L. Möller, I. Kang, and A. J. van Wijngaarden, "Experimental Demonstration of Broadband PMD Mitigation Through Distributed Fast Polarization Scrambling and FEC," Proc. 30th Eur. Conf. on Optical Commun. (ECOC '04) (Stockholm, Swed., 2004), paper Th4.1.4.
[36] X. Liu, C. Xie, and A. J. van Wijngaarden, "Multichannel PMD Mitigation Through Forward-Error-Correction With Distributed Fast PMD Scrambling," Proc. Optical Fiber Commun. Conf. (OFC '04) (Los Angeles, CA, 2004), vol. 2, paper WE2.
[37] A. J. Lowery, L. Du, and J. Armstrong, "Orthogonal Frequency Division Multiplexing for Adaptive Dispersion Compensation in Long Haul WDM Systems," Proc. Optical Fiber Commun./National Fiber Optic Engineers Conf. (OFC/NFOEC '06) (Anaheim, CA, 2006), paper PDP39.
[38] D.-S. Ly-Gagnon, S. Tsukamoto, K. Katoh, and K. Kikuchi, "Coherent Detection of Optical Quadrature Phase-Shift Keying Signals With Carrier Phase Estimation," J. Lightwave Technol., 24:1 (2006), 12–21.
[39] L. Möller, J. H. Sinsky, H. Haunstein, S. Chandrasekhar, C. R. Doerr, J. Leuthold, C. A. Burrus, and L. L. Buhl, "Higher Order PMD Distortion Mitigation Based on Optical Narrow Bandwidth Signal Filtering," IEEE Photonics Technol. Lett., 14:4 (2002), 558–560.
[40] M. Nakamura, H. Nosaka, M. Ida, K. Kurishima, and M. Tokumitsu, "Electrical PMD Equalizer ICs for a 40-Gbit/s Transmission," Proc. Optical Fiber Commun. Conf. (OFC '04) (Los Angeles, CA, 2004), vol. 1, paper TuG4.
[41] C. D. Poole, "Measurement of Polarization-Mode Dispersion in Single-Mode Fibers With Random Mode Coupling," Optics Lett., 14:10 (1989), 523–525.
[42] C. D. Poole and J. Nagel, "Polarization Effects in Lightwave Systems," Optical Fiber Telecommunications, Vol. IIIA (I. P. Kaminow and T. L. Koch, eds.), Academic Press, San Diego, CA, 1997, pp. 114–161.
[43] J. Renaudier, G. Charlet, M. Salsi, O. B. Pardo, H. Mardoyan, P. Tran, and S. Bigo, "Linear Fiber Impairments Mitigation of 40-Gbit/s Polarization-Multiplexed QPSK by Digital Processing in a Coherent Receiver," J. Lightwave Technol., 26:1 (2008), 36–42.
[44] D. Sandel, M. Yoshida-Dierolf, R. Noé, A. Schöpflin, E. Gottwald, and G. Fischer, "Automatic Polarisation Mode Dispersion Compensation in 40 Gbit/s Optical Transmission System," Electronics Lett., 34:23 (1998), 2258–2259.
[45] S. J. Savory, A. D. Stewart, S. Wood, G. Gavioli, M. G. Taylor, R. I. Killey, and P. Bayvel, "Digital Equalisation of 40 Gbit/s per Wavelength Transmission Over 2480 km of Standard Fibre Without Optical Dispersion Compensation," Proc. 32nd Eur. Conf. on Optical Commun. (ECOC '06) (Cannes, Fr., 2006), paper Th2.5.5.
[46] W. Shieh and C. Athaudage, "Coherent Optical Orthogonal Frequency Division Multiplexing," Electronics Lett., 42:10 (2006), 587–589.
[47] W. Shieh, X. Yi, Y. Ma, and Y. Tang, "Theoretical and Experimental Study on PMD-Supported Transmission Using Polarization Diversity in Coherent Optical OFDM Systems," Optics Express, 15:16 (2007), 9936–9947.

[48] H. Sunnerud, C. Xie, M. Karlsson, R. Samuelsson, and P. A. Andrekson, "A Comparison Between Different PMD Compensation Techniques," J. Lightwave Technol., 20:3 (2002), 368–378.

[49] B. Wedding and C. N. Haslach, "Enhanced PMD Mitigation by Polarization Scrambling and Forward Error Correction," Proc. Optical Fiber Commun. Conf. (OFC '01) (Anaheim, CA, 2001), vol. 3, paper WAA1-1.

[50] C. Xie, S. Chandrasekhar, X. Liu, D. Werner, and H. Haunstein, "Automatic Optical PMD Compensator for 40-Gb/s DBPSK and DQPSK With Fast Changing SOP and PSP," Proc. 34th Eur. Conf. on Optical Commun. (ECOC '08) (Brussels, Belg., 2008), paper We.3.E.5.

[51] C. Xie and H. Haunstein, "Optimum Length of One-Stage Polarization-Mode Dispersion Compensators With a Fixed Delay Line," IEEE Photonics Technol. Lett., 15:9 (2003), 1228–1230.

[52] C. Xie, X. Liu, and H. Bülow, "PMD-Induced Outage Probability in an Optical Communication System With Fast Polarization Scramblers and Time-Varying PMD Sections," IEEE Photonics Technol. Lett., 20:6 (2008), 440–442.

[53] C. Xie and L. Möller, "Comparison of Different Feedback Signals for One-Stage Polarization-Mode Dispersion Compensators," IEEE Photonics Technol. Lett., 17:3 (2005), 570–572.

[54] C. Xie, L. Möller, H. Haunstein, and S. Hunsche, "Comparison of System Tolerance to Polarization-Mode Dispersion Between Different Modulation Formats," IEEE Photonics Technol. Lett., 15:8 (2003), 1168–1170.

(Manuscript approved July 2008)

HENNING BÜLOW is a member of technical staff in the

Optical Networks Department at Bell Labs in Stuttgart, Germany. He received his Dipl.-Ing. degree in electrical engineering from the University of Dortmund, Germany, and a Ph.D. in electrical engineering from the University of Berlin for work on integrated optical switching matrices. During his 18 year tenure with Alcatel-Lucent Bell Labs and formerly with its Research and Innovation Division, he has worked on erbium-doped fiber amplifiers, on the assessment of data transmission in the presence of polarization mode dispersion, and on dynamic mitigation of transmission impairments at channel rates beyond 10 Gb/s by adaptive analog and digital electronic equalizer circuits and optical signal processing. He has authored or co-authored more than 110 conference and journal contributions, written three book chapters, holds more than 50 patents, and has served on the technical program committee of the Optical Fiber Communication Conference and Exposition (OFC). He is also currently serving as Guest Professor with the University of Erlangen-Nuremberg.

CHONGJIN XIE is a member of technical staff in the

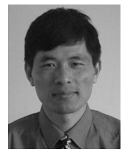

Optical Transmission Systems and Networking Department at Bell Labs in Holmdel, New Jersey. He received his M.Sc and Ph.D degrees from Beijing University of Posts and Telecommunications. Prior to joining Bell Labs, he conducted postdoctoral research at the Photonics Laboratory at Chalmers University of Technology in Sweden. During his tenure with Bell Labs, his research interests have encompassed fiber optical communication systems and networks including high-speed lightwave transmission, polarization mode dispersion, polarization dependent loss, modulation formats, and optical performance monitoring. He has authored and co-authored more than 120 journal and conference papers and holds eight patents.

AXEL KLEKAMP is a member of technical staff in the

Optical Networks Department at Bell Labs in Stuttgart, Germany. He received his Ph.D. in physics from the University of Stuttgar, and shortly thereafter joined Alcatel's Research and Innovation Division in Stuttgart, where he was engaged in experimental and theoretical work on photonic components. During his 16 year tenure, he has worked on modeling, design, and layout of large-scale and high-density passive optical components (planar lightwave circuits) and their applications to advanced optical transmission systems. He has been with the Optical Transmission Group for the past six years and is currently working on optical transmission at high data rates (10 Gb/s to 100 Gb/s). His current research interests include transmission system tolerance analysis and impairment mitigation, modulation formats, and performance monitoring. He has authored and co-authored more than 50 journal and conference papers and holds five patents.

XIANG LIU is a member of technical staff in the Optical Transmission Systems and Networking Department at Bell Labs in Holmdel, New Jersey. He received an M.S. degree in physics from the Institute of Physics, Chinese Academy of Sciences, and a Ph.D. degree in applied physics from Cornell University, Ithaca, New York. His doctoral work contributed to the first generation of optical spatiotemporal solitons. His current research interests include coherent optical OFDM, high-speed optical transmission, novel nonlinearity and dispersion management, mitigation of polarization-mode dispersion, and analytical and numerical modeling of optical transport systems. He has authored and co-authored more than 150 journal and conference papers and holds 25 U.S. patents.

BERND FRANZ is a member of technical staff in the Optical Networks Department at Bell Labs in Stuttgart, Germany. He received his Dipl.-Ing. degree in electrical engineering from the University of Braunschweig, Germany. He has been with Alcatel-Lucent Bell Labs, and formerly with its Research and Innovation Division in Stuttgart, Germany, for 21 years . His current research interests include high-speed optical transmission, and in particular electronic distortion equalization. He has authored more than 50 journal and conference papers and holds more than ten international patents. ◆